JOURNAL OF THE ROYAL SOCIETY Interface

J. R. Soc. Interface (2010) **7**, 1627–1639
doi:10.1098/rsif.2010.0126
Published online 4 August 2010

Spatial dynamics of bar-headed geese migration in the context of H5N1

L. Bourouiba[1,*], Jianhong Wu[2], S. Newman[3], J. Takekawa[4], T. Natdorj[5], N. Batbayar[6], C. M. Bishop[7], L. A. Hawkes[7], P. J. Butler[8] and M. Wikelski[9]

[1]*Department of Mathematics, Massachusetts Institute of Technology, 77 Massachusetts Avenue, Cambridge, MA 02139, USA*
[2]*Centre for Disease Modeling, York University, 47000 Keele Street, Toronto, ON, Canada M3J 1P3*
[3]*United Nations Food and Agriculture Organization, EMPRES Wildlife Unit, Emergency Centre for Transboundary Animal Diseases, Animal Production and Health Division, Rome 00153, Italy*
[4]*U.S. Geological Survey, Western Ecological Research Center, 505 Azuar Drive, Vallejo, CA 94592, USA*
[5]*Institute of Ornithology, Mongolian Academy of Sciences, Ulaanbaatar 210351, Mongolia*
[6]*Wildlife Science and Conservation Center, Undram Plaza 404, Bayanzurkh District, Ulaanbaatar 210351, Mongolia*
[7]*Bangor University, School of Biological Sciences, Bangor, Gwynedd LL57 2UW, UK*
[8]*School of Biosciences, University of Birmingham, Birmingham B15 2TT, UK*
[9]*Max Planck Institute for Ornithology, Schlossallee 2, Radolfzell, Germany*

Virulent outbreaks of highly pathogenic avian influenza (HPAI) since 2005 have raised the question about the roles of migratory and wild birds in the transmission of HPAI. Despite increased monitoring, the role of wild waterfowl as the primary source of the highly pathogenic H5N1 has not been clearly established. The impact of outbreaks of HPAI among species of wild birds which are already endangered can nevertheless have devastating consequences for the local and non-local ecology where migratory species are established. Understanding the entangled dynamics of migration and the disease dynamics will be key to prevention and control measures for humans, migratory birds and poultry. Here, we present a spatial dynamic model of seasonal migration derived from first principles and linking the local dynamics during migratory stopovers to the larger scale migratory routes. We discuss the effect of repeated epizootic at specific migratory stopovers for bar-headed geese (*Anser indicus*). We find that repeated deadly outbreaks of H5N1 on stopovers during the autumn migration of bar-headed geese could lead to a larger reduction in the size of the equilibrium bird population compared with that obtained after repeated outbreaks during the spring migration. However, the opposite is true during the first few years of transition to such an equilibrium. The age-maturation process of juvenile birds which are more susceptible to H5N1 reinforces this result.

Keywords: avian influenza H5N1; modelling; satellite tracking; bar-headed geese

1. INTRODUCTION

Outbreaks of highly pathogenic avian influenza (HPAI) H5N1 have led to the culling of hundreds of millions of domesticated birds since 2003 (e.g. Stöhr 2005). To date human death cases due to H5N1 account for a cumulative number of more than 400 victims worldwide, most were in contact with poultry prior to diagnosis (Center for Infectious Disease Research & Policy 2009; World Health Organization 2009*a*,*b*). Despite the increasing number of human victims, the identification of cases of human-to-human transmission remains rare (Ungchusak *et al.* 2005; World Health Organization 2008). However, the prospect of human-to-human transmission leading to a major pandemic is at the origin of the intensive monitoring of flu outbreaks around the world in the last decade.

Cases of H5N1 have been inducing outbreaks and death among various wild animal species since the 1990s. Birds of the order of Anseriformes (e.g. ducks, geese and swans) and Charadriiformes (e.g. gulls, terms and waders) are generally considered to be the

*Author for correspondence (lydia.bourouiba@math.mit.edu).
Author contributions: L. Bourouiba and J. Wu initiated, designed, performed the research, and wrote the paper. S. Newman, J. Takekawa, T. Natdorj, N. Batbayar, C. M. Bishop, L. A. Hawkes, P. J. Butler, and M. Wikelski contributed migration ecology information on bar-headed geese and provided context for that information.

Electronic supplementary material is available at http://dx.doi.org/rsif.2010.0126 or via http://rsif.royalsocietypublishing.org.

Received 4 March 2010
Accepted 21 April 2010

avian influenza virus reservoir in nature (Webster *et al.* 1992; Olsen *et al.* 2006). Although various definitions of reservoir are possible (Haydon *et al.* 2002), here we use 'reservoir' in order to refer to the bird groups showing relatively low mortality and mild symptoms when infected, and without which the sustainability and spread of the virus into human and domestic bird target populations would not be possible. In 2005, a new highly pathogenic H5N1 strain led to an anomalously high cumulative mortality of more than 6000 wild birds in central China's Qinghai Lake (Chen *et al.* 2005). Among other species, the casualties included 3018 bar-headed *(Anser indicus)* geese (Zhou *et al.* 2006) representing 5–10% of the global population (Javed *et al.* 2000; Prins & van Wieren 2004; Olsen *et al.* 2006; Avian Influenza Wildlife & The Environment Web 2008; Bird Life International 2009). This hecatomb was followed by other deadly outbreaks among wild birds in Russia, Mongolia, India, the Middle East, Europe and Africa. The H5N1 virus is now endemic in poultry and local birds in several regions of the world (Chen *et al.* 2004; Center for Infectious Disease Research & Policy 2008). The conditions favourable for the H5N1 endemicity are still not well understood and remain controversial. In fact, following the deadly outbreaks of 2005, migratory birds were designated as the source and disseminator of H5N1. In particular, they were thought of as the cause of contamination of poultry. This hypothesis was quickly adopted by various organizations such as the World Health Organization (2005). Some studies supported this hypothesis, declaring finding H5N1 virus in the excretion of sampled wild birds (Chen *et al.* 2005, 2006*a*,*b*; Liu *et al.* 2005; Lipatov *et al.* 2007). However, the methodology used in these studies has been questioned on several occasions (e.g. Feare & Yasué 2006; Yasué *et al.* 2006; Weber & Stilianakis 2007) based on the issues related to improper identification of the birds sampled, unreported location of capture and possible bias of the sampling itself. The critical authors argued that the lack of precise identification of captured birds did not allow one to conclude on whether the birds sampled were part of a regional or migratory sub-species, whether they were wild or domesticated and, hence, whether they might have been exposed to the virus during migration or locally in nearby farms and shared water bodies.

Low pathogenic avian influenza (LPAI) viruses were previously thought to impart no symptoms to wild birds. Hence, birds were thought of as spreaders of these strains, allowing them to travel over long migratory distances. However, van Gils *et al.* (2007) captured and monitored migratory Bewick swans (*Cygnus columbianus bewikii*) in their natural environment and found that the feeding and migratory performance of LPAI-infected birds were altered. In fact, infected birds showed reduced bite and fuel storage rates and delayed migratory schedule when compared with their healthy counterparts. Hasselquist *et al.* (2007) studied the flight behaviour of red knot (*Calidrus canutus*) in a wind tunnel and found that long flight did not appear to influence immune responses. However, some birds with low antibody response against tetanus refused to take off. This suggested that only birds in sufficiently good health engage in the demanding physical activity of migration. Some domestic birds infected with LPAI viruses showed respiratory symptoms, depression and egg production problems (Alexander 2000). The consequences of these findings on the effect of LPAI on wild birds were discussed in van Gils *et al.* (2007), where the authors note that the infected birds with reduced bite and fuel storage rates could have delayed departure from all subsequent stopovers. In turn, this accumulated delay could reduce the likelihood of the bird finding advantageous unoccupied breeding territories and result in reduced reproductive output (Kokko 1999). In addition, the delay in reproduction could hinder the late broods to take full advantage of the peak of nutrient availability (Both & Visser 2005). These recent findings on the low pathogenic strain of avian influenza called for a paradigm shift and a forced re-evaluation of the attributed role of wild birds as the main spreaders of the lethal highly pathogenic strains.

The chain of transmission of the highly pathogenic H5N1 strain involves a complex interplay of wild bird movement, poultry trade and their interaction with many local or migratory, wild or domesticated other species. For example, carnivorous animals (e.g. cats and foxes) fed with carcasses of infected dead birds or poultry were observed to excrete the virus. Although infected cats showed symptoms and were able to cause horizontal disease transmission, foxes showed little symptoms (e.g. Kuiken *et al.* 2004; Reperant *et al.* 2008). Focusing on wild birds and poultry movements and using a set of 52 H5N1 introduction events worldwide, Kilpatrick *et al.* (2008) estimated that the likelihood of poultry trade to be the cause of H5N1 introduction events was three times as high as migratory bird movement in Asia. However, the opposite was true for Europe, where migratory bird movement was found to be the most likely cause of the introduction of H5N1. To our knowledge, only one study documented movement (over several hundred kilometers) of a migratory wild bird infected with a highly pathogenic avian influenza (Gaidet *et al.* 2008). A more recent study examining the role of migratory common teal in spreading the virus in Europe did not show a strong link between the two (Lebarbenchon *et al.* 2009). The study was based on an individual-based model with explicit spatial location. In short, the mechanisms of worldwide spread of H5N1 remain unclear.

The possible indirect infection of domesticated and wild animals in local communities collocated with poultry farming or migratory stopovers illustrates the complexity of the chain of transmission of H5N1. Thus, it appears to be important to incorporate local dynamics of the stopovers along bird migratory routes when modelling the spread of HPAI. In fact, the local dynamics on migratory stopovers appears critical not only to the understanding of the onset of an outbreak in some geographical locations, but also to understanding the ecological impact of endemicity of H5N1 in certain regions where susceptible migratory birds stop. This last aspect is one focus of our study, where the spatial modelling of the seasonal migration of bar-headed

geese is presented. We chose to focus on bar-headed geese as example species due to their vulnerability to H5N1, as highlighted by the death toll in the 2005 Qinghai Lake outbreak. In addition, the path of migration of this species is known to pass through a succession of areas where H5N1 is now endemic. These data allowed us to capture the key temporal and spatial scales characteristic of the migration of bar-headed geese.

Seminal works on the modelling of bird migration include the study of Weber *et al.* (1998), who used a stochastic optimization model where birds going through a succession of stopover sites had to choose their migration schedule and fuelling to maximize their reproductive success. Barta *et al.* (2008) focused on the 1-year annual cycle in a seasonal environment using an optimization model where female birds choose an action among reproduction, foraging, moulting or migrating. Bauer *et al.* (2008) investigated the effect of climate-influenced conditions of stopover sites on the schedule of migration for pinkfooted geese, where an optimization model was also used. Dolman & Sutherland (1994) used a population model combining foraging ecology with population biology in order to examine the response of migratory and non-migratory birds to habitat loss. Although these studies attempted to model bird migration, they did not link the local and non-local dynamics of disease spread to migratory birds. More recent studies aiming at linking disease spread and migration include Kilpatrick *et al.* (2008) and Lebarbenchon *et al.* (2009). There are also some recent spatio-temporal correlation-type studies aimed to examine the correlation between the presence of migratory birds in a given location and H5N1 outbreaks (e.g. Gilbert *et al.* 2006; Si *et al.* 2009). However, these studies do not address the causality between bird migration and spread of H5N1: neither the impact of bird migration on the spread of avian influenza nor the impact of influenza outbreaks on the migratory bird populations is addressed. As a result, the key aspects of bird population dynamics and the impact of repeated outbreaks on stopovers where HPAI is endemic remain unknown.

In this study, we present a seasonal migration model incorporating both the population dynamics of the birds and the local disease dynamics on stopover sites along the migratory route. The aim of the study is to capture the key links between the population dynamics of the migratory species and the disease endemicity at various points along the migratory routes. We note that the local dynamics of migratory stopovers can involve interactions and cross-contamination between local domesticated birds, local poultry industry and temporary migratory birds residing in the community. However, we start by introducing the impact of H5N1 virus on various stopovers in a simple manner, with the aim to pave the way to a more complete incorporation of disease dynamics in migration models. Indeed, a repeated massive death toll of birds due to H5N1 could have major ecological implications for the long-term dynamics of the species. Hence, we present a model coupling the seasonal migration with the population and disease dynamics on stopovers in order to assess the overall impact of repeated H5N1 outbreaks on the ecology of the migratory birds considered. The proposed model is analysed both mathematically and numerically using data on bar-headed geese. The implications of the results obtained for the conservation and population dynamics of the species are discussed. Finally, a preliminary numerical assessment of the effect of age maturation of the young birds on the species dynamics is also discussed.

2. METHODS

2.1. Formulation of the mathematical model of bird migration

The factors determining the onset and trajectories involved in bird migration are complex and are the subject of active research. Most migratory birds are observed to return yearly to some known stopovers, breeding and wintering sites (Akesson & Hedenström 2007). Despite the complexity of their migratory routes, birds are observed to follow similar migration paths yearly (Alerstam 2006). Their trajectories are schematically represented on Mercator projection maps as curved loops with different spring and autumn arcs. However, whether migratory birds follow orthodromes (great circle route) or loxodromes (rhumb line route) or a combination of both remains unclear (Gudmundsson & Alerstam 1998). In fact, orthodromes are lines of shorter distance on a sphere (appearing curved on Mercator projection maps) which could be more energetically efficient (Akesson & Hedenström 2007); however, other factors such as winds and major geographical barriers (e.g. Sahara and Himalayas) could be even more significant in defining the path of minimum migratory energy (Alerstam 2006). Satellite tracking of birds now provides a valuable asset in helping to identify migratory trajectories and the factors influencing their change. For example, satellite tracking of ospreys between Europe and West Africa led to the identification of larger variation of departure times in the autumn compared with the spring migration, with a higher emphasis on short migration during the spring explained by the higher reproductive pressure at the end of this season. However, key stopovers were shared and persistent from one year to the next (Alerstam *et al.* 2001). More recently, using satellite tracking, migration paths of a dozen bar-headed geese were recorded (author's unpublished data). The yearly migratory routes of birds were reported on a Mercator projection map and were observed to approximately follow curved routes as seen in figure 1. Note that the model depiction does not necessarily imply a circular migration. Not all bar-headed geese breed at the same place. In fact, sub-groups of bar-headed geese breed in central China (e.g. Qinghai Lake area) or even in the Tibet area (Javed *et al.* 2000; Takekawa *et al.* 2010). We followed the recorded trajectories of a few of the tracked birds that clearly departed from the north-most breeding ground located in Mongolia and arrived in a wintering ground located in northwest India as discussed in §2.2.

We represent the migratory route by a continuous two-dimensional spatial domain consisting of a succession of elongated flight channels and stopover regions

(patches) of small scales compared with the length of the connecting flyways. This approach accounts for the flow at the cross section of the channel, where we neglect the transversal fluctuations of the bird flight velocities. The underlying assumption of this approach is the continuity in the flow of birds in the air. The interaction between the birds, distance between departing flocks and the aerodynamics of the arrangement of birds within a flock or the distance between flocks are not accounted for in this model. The schematic diagrams for the formulation of the model are given in figure 2. The patches are stopover locations, where resources/virus can be shared/transmitted. A succession of $N+1$ stopover regions of surfaces S_n is denoted by P_n with $0 \leq n \leq N$. We consider the patches to be of small scale when compared with the overall migratory path, i.e. $\epsilon \ll L$. In addition, we assume the patches to be circular with radius ϵ, leading to $\int_{\partial Pn} dy = \text{arc} = \epsilon\theta$, with $\theta = 2\sin^{-1}(l/2\epsilon)$. Assuming $\epsilon \gg l$, then arc $\approx l$, otherwise, considering a smaller patch radius of, for example, $\epsilon = l/2$ (as shown in figure 2) leads to $\int_{\partial Pn} dy = \pi\epsilon = \pi l/2 \approx l$.

In our model, we consider a fixed cycle of migration where routes for the autumn and spring migration are distinct, and we assume that the birds share the main stopover locations. Indeed, as discussed in more detail in §2.2, the data revealed that some of the main stopovers are common to tracked birds (for example, a water point before the longest journey across the Himalayas), while others were not. Note that for some species and sub-groups of birds within a species some of the stopovers are observed to be common to the fall and spring migration as well. Our model can easily account for some coinciding patches in the fall and spring if needed. Here, we consider the direction of a flock trajectory to be parallel to the virtual contour representing the channel of various geometries in which migratory birds flow. In a natural coordinate, we have x, the direction along the boundaries of the route, and y, the normal away from the centre of curvature. The length of the closed migratory domain in the tangential direction x is L. The fixed width of the channel in the y direction is l ($L \gg l$) and $\bar{\rho}(x, y, t)$ is the density of the birds. The length of the flyway between two patches P_n centred around x_n and patch P_{n+1} centred around x_{n+1} is $d_{n,n+1} = |x_{n+1} - x_n - 2\epsilon|$. U is the average longitudinal velocity of the flocks between stopovers. We consider the cross section of the channel to be small in comparison with the length of the channel in the x-direction and that $\partial\bar{\rho}/\partial x \gg \partial\bar{\rho}/\partial y$; hence, the density is considered uniform in the y-direction of the flyway. We thus denote by $\bar{\rho}(x,y,t) \approx \rho(x,t)$ in the flyways. In the channel, the number of birds passing a given element cross section dy per unit time is $U\rho(x,t)\mathbf{n}dy$, where $\mathbf{n}$ is the unit outward normal to the cross section dy. The seasonality of the migration is taken into account in concordance with the bird location. When the spring migration is initiated, the departure patch P_0 is the southern-most stopover region centred around $x_0 = 0$. It is adjacent to the last wintering P_N centred around $x_N{=}L$. Patch $P_{N/2}$ is the northern-most breeding ground, where birds spend the summer. The birds spend T_w days in the wintering region P_N, T_s days performing their spring migration from P_0 to $P_{N/2}$, after which they reside in the breeding location ($P_{N/2}$) for T_b days, before undertaking their autumn migration for T_f days towards the wintering ground P_N. The derivation of the conservation of number of birds in the flyways between two patches P_n and P_{n+1} leads to a continuity equation similar to that derived for mass conservation in hydrodynamics (see the electronic supplementary material). It is equivalent to a Lagrangian conservation of bird density with $d\rho/dt = 0$; hence, a flock of birds travelling at speed U_n with an initial density $\rho_{n-1} = \rho(x_{n-1} + \epsilon, t_{n-1})$ at the interface of patch P_{n-1} at time t_{n-1} conserves its density along its trajectory and arrives at the interface of patch P_n at $x_n - \epsilon$ at time t_n with a density $\rho(x_n - \epsilon, t_n) = \rho(x_{n-1} + \epsilon, t_{n-1})$. The departure and arrival times are related by $t_{n-1} = t_n - d_{n-1,n}/U_n$, leading to $\rho(x_n - \epsilon, t_n) = \rho(x_{n-1} + \epsilon, t_n - \tau_n)$, where $\tau_n = d_{n-1,n}/U_n$. Considering a constant uniform departure rate *per capita* m_n on patch P_{n-1}, we obtain the total departure rate at time t_{n-1} as $\int_{\partial P_{n-1}} U_n\rho(x_{n-1} + \epsilon, t_{n-1})dy = \int_{P_{n-1}} m_n\bar{\rho}(x, y, t_{n-1})dx\,dy = m_nS_{n-1}M^{n-1}(t_{n-1})$, where $M^{n-1}(t) = \int_{P_{n-1}} \bar{\rho}(x, y,t)dx\,dy/S_{n-1}$ is the average density of birds on patch P_{n-1} and ∂P_{n-1} corresponds to the cross section linking patch and flyway. $\int_{\partial P_n} dy \approx l$ is the width of the flyway. Hence, we can relate the number of birds leaving patch P_{n-1} at t_{n-1} per unit time to those entering patch P_n at t_n with $\rho(x_n - \epsilon, t_n) = m_nS_{n-1}M^{n-1}(t_n - \tau_n)$. If a constant death rate $\bar{\mu}_i$ along the flyway linking patches P_{i-1} to P_i is assumed, we obtain a simple modification of the equations (see the electronic supplementary material). We then can proceed in expressing the rate of change of the number of birds $S_nM^n(t)$ on a patch P_n. On each patch, the number of birds is affected by the incoming and outgoing flux of birds and the local death rates μ_n. Assuming that all patches have approximately the same surface areas, we can reduce the equation on the number of birds to an equation on the average density on patch P_n as the following system of delay differential equations:

$$\begin{aligned}
\dot{M}^0(t) &= e^{-\bar{\mu}_0\tau_0} m_0(t-\tau_0)M^N(t-\tau_0) \\
&\quad - (m_1 + \mu_0)M^0(t), \\
\dot{M}^1(t) &= e^{-\bar{\mu}_1\tau_1} m_1M^0(t-\tau_1) - (m_2 + \mu_1)M^1(t), \\
&\vdots \\
\dot{M}^{N/2}(t) &= e^{-\bar{\mu}_{N/2}\tau_{N/2}} m_{N/2}M^{N/2-1}(t-\tau_{N/2}) \\
&\quad + \gamma M^{N/2}(t)\left(1 - \frac{M^{N/2}(t)}{K}\right) \\
&\quad - m_{N/2+1}(t)M^{N/2}(t), \\
&\vdots \\
\text{and}\quad \dot{M}^N(t) &= e^{-\bar{\mu}_N\tau_N} m_NM^{N-1}(t-\tau_N) \\
&\quad - (m_0(t) + \mu_N)M^N(t),
\end{aligned} \tag{2.1}$$

where the birth rate is modelled using a logistic growth model accounting for the limiting-carrying capacity of N_{max} number of birds and the intrinsic

Figure 1. Examples of autumn migratory route from satellite tracking of bar-headed geese BH08-82098, BH08-41592 and BH08-41720 (produced using Google Earth 2009).

growth rate of γ and where the density-carrying capacity is $K = N_{\max}/S_{N/2}$. Patches P_0 and P_N are assumed to be adjacent and $\tau_0 = 0$ in the remainder of the study of this model. The departure coefficients m_n with $0 \leq n \leq N$ are assumed to be all positive constants, except for $m_0(t)$ and $m_{N/2+1}(t)$ which are T-periodic positive functions, with $T = T_w + T_s + T_b + T_f = 365$ days. The well-posedness and threshold dynamics of this system are detailed in the electronic supplementary material.

2.2. Parameters

The parameters to be used are summarized in Tables 1 and 2. Death rates in the wild are difficult to obtain; however, an estimate of 0.55–0.9 survival probability from one year to the next was given for geese in Schekkerman & Slaterus (2007), depending on the body mass of the birds considered. In the first part of our simulations, juveniles are not distinguished from the rest of the birds and we consider an average survival of 0.725 of the population during the autumn migration and on flight. We consider the winter and spring migrations to have higher death rates than those of the autumn and summer. This is due to both the higher survival rate of various viruses in colder temperatures (e.g. Brown *et al.* 2007, 2009) and the scarcity of the resources for refuelling on the stopovers along the spring migration in comparison with the autumn migration (Ward *et al.* 1997). Note that this hypothesis only accounts for natural death and could be jeopardized when considering species heavily hunted during the autumn (e.g. Madsen *et al.* 2002). The notion that birds would follow a 'green wave' of highly nutritional early growing plants is not incorporated here due to the difficulty in comparing the nutritional intake during the spring versus autumn migrations. Hence, in this first part we consider the winter and spring migration to have higher death rates than those of the fall and summer; however, in the second part of the paper we account for the higher death rate of juveniles and their increased numbers in the summer and fall. This is done by incorporating demographics with group-specific mortality rates.

From the satellite tracking data of bar-headed geese (fall migration 2008 and early spring migration 2009) and other data reported in Javed *et al.* (2000) for another group of bar-headed geese, we focused on the longest southward migratory paths (from Mongolia to India) and we chose not to use the data of the birds for which the tracking was interrupted. From the remaining data, we extracted the date of arrival, the length of stay and the date and time since deployment in Mongolia. The average distance and time of flight between the current and previous stop sites were also extracted. The duration of flight and residence on the stopovers varied from days to up to a month in rare cases. This appeared to be due to geographical considerations including the location of the water points and obstacles such as the Himalayas. Based on these data,

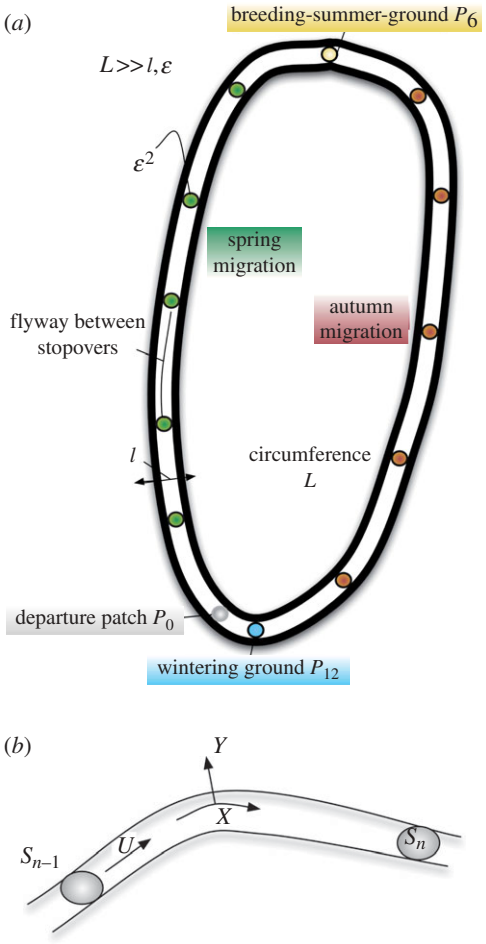

Figure 2. Schematic illustrations of (*a*) the migratory channel model with five stopovers on each of the autumn and spring migration routes and (*b*) the local frame used in the derivation of the equation in the flyways linking patches.

we estimated the total number of stopovers, the average flight time and the average speed between stopovers based on the following considerations. After the onset of migration in Mongolia, we chose to discard the stopovers where the birds remained for less than a day and those located at less than 100 km from the previous reported stopover. In fact, some birds appeared to fly back and forth in restricted areas a few dozen kilometres away from their original stop. We chose to not account for these local 'hops' in the data reporting migration stopovers. As a result, the data of the bar-headed geese tracked led to the identification of an average of five stopovers during the autumn migration and we then assumed the same number of stops along the spring migration. The longest distance travelled continuously was of the order of ≈ 700 km in a few days at a speed of up to $\approx 11\ \mathrm{m\,s^{-1}}$ (BH08-41592) to cross the Himalayas. Elsewhere the birds stopped more frequently and flew at slower speeds, with an average velocity of $1.98\ \mathrm{m\,s^{-1}}$ for the birds considered ($2.12\ \mathrm{m\,s^{-1}}$ BH08-41592, $0.95\ \mathrm{m\,s^{-1}}$ BH08-41720, $1.84\ \mathrm{m\,s^{-1}}$ BH08-82098 and $3\ \mathrm{m\,s^{-1}}$ no. 11753). The time in flight between stopovers was also averaged between birds and their stopovers, leading us to the delay of $\tau = 2.6$ days. Note that we excluded the delay recorded for BH08-41720 as details on the stopover locations were not all accessible. Note that the birds stayed for a longer time in one to two preferential stopover areas close to the breeding patch before departing for the autumn migration. These long stopovers in the early stage of the autumn migration could be explained by the clement weather in late September and early October when they finish moulting (Cui *et al.* 2010). Based on these numbers, we discuss the model of patches P_0 to P_{12} with longer stopover durations during the autumn migration compared with that of the spring and with migration parameters in table 1.

Table 1. Departure rates for the stopover patches along spring and autumn migrations. The departure coefficient m is calculated to estimate the departure of 99.99% of the birds after the number of days indicated in the middle column. Note that P_0 is a transition departure location, where birds stay only briefly. The birds reside up to 138 days on P_6, after which 99.99% of birds are assumed to leave over 1 day. Similarly, for P_{12}, where birds reside for 120 days before almost all leaving for P_0 over 1 day. The average duration of flight between two stopovers is $\tau = 2.6$ days (see text). The average residence time on each stopover along the migrations (excluding the breeding, wintering and departure patches) is 7.58 days and corresponding $m_{\mathrm{average}} = 0.60754$.

patch n	residence (in days)	m_{n+1}
P_0 departure	1	9.21034 (m_1)
spring migration		
P_1	2.2	2.09326 (m_2)
P_2	13	0.35424 (m_3)
P_3	5	0.92103 (m_4)
P_4	8	0.57565 (m_5)
P_5	2.2	2.09326 (m_6)
P_6 breeding	138 days	9.21034 ($\bar{m}_{N/2+1}$)
autumn migration		
P_7	15	0.30701 (m_8)
P_8	10	0.46052 (m_9)
P_9	6.4	0.71956 (m_{10})
P_{10}	6	0.76753 (m_{11})
P_{11}	8	0.57565 (m_{12})
P_{12} wintering	120 days	9.21034 ($\bar{m}_0$)

Concerning the parameters related to the disease induced death rates, recall that the 2005 epizootic in central China's Qinghai Lake led to a death toll of more than 6000 wild birds of various species (Chen *et al.* 2005) among which 3018 were bar-headed geese. The strains of H5N1 involved would cause the death of 80 per cent of the inoculated geese (for three week-old juvenile geese from eastern Zhejiang) within 8.7–12.9 days post-inoculation in Zhou *et al.* (2006). In Brown *et al.* (2008), two out five died in a similar period of time (bar-headed geese of $\approx$12 weeks). Assuming the 80 per cent death rate within an average time of 11 days, we deduce a disease induced death rate of 1.46×10^{-1} per day.

3. RESULTS

3.1. One-age group model

Figure 3 shows the periodic seasonal migration functions $m_0(t)$ and $m_{N/2+1}(t)$ used for the simulations of

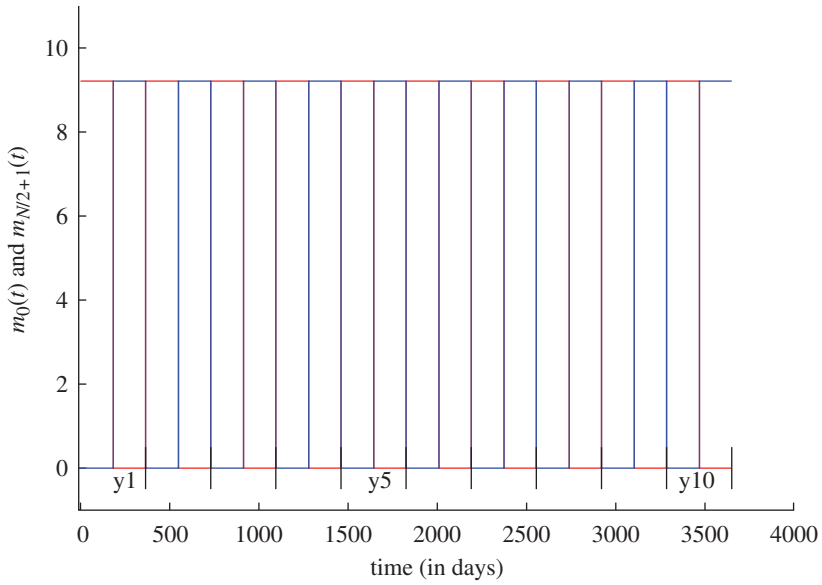

Figure 3. Migration cycle functions $m_0(t)$ (red line) and $m_{N/2+1}(t)$ (blue line) controlling the initiation of the spring and autumn migration, respectively. The years of 365 days are indicated with the labels y1 to y10 for year 1 to year 10.

Table 2. Parameters of the model for the case of bar-headed geese. The determination of the seasonality and migration durations were done based on the data collected in Javed *et al.* (2000), Prins & van Wieren (2004) and the satellite tracking of the geese nos. BH08-82098, BH08-41592 and BH08-41720.

spring migration	15 March–April, $T_s = 46$ days
breeding ground	May–15 September, $T_b = 138$ days
autumn migration	15 September–15 November, $T_f = 61$ days
wintering ground	15 November–15 March, $T_w = 120$ days
number of stopovers	major stopover locations recorded
BH08-41592	5 (autumn Mongolia-to-India)
BH08-82098	5 (autumn Mongolia-to-India)
BH08-41720	6 (autumn Mongolia-to-India)
goose no. 11753	2 (spring India-to-China Lunggar) (Javed *et al.* 2000)
world population	30 000–60 000 (Javed *et al.* 2000; Prins & van Wieren 2004; Olsen *et al.* 2006; Bird Life International 2009)
female/male ratio	more females than males, this ratio varies, e.g. 1–1.4 in April in captivity (Lamprecht 1987) or in wild (Prins & van Wieren 2004); we assumed 55–45% (1.2 ratio)
egg laying	average 5.3 eggs per mature female with 34% average hatching (Wurdinger 1973)
γ	4.99×10^{-3} per day (during 138 days of breeding season)
K	60 000
annual survival rate (ASR)	0.55–0.9 (average of 0.725) depending on body mass (Schekkerman & Slaterus 2007)
life expectancy	15–20 years, we chose 17 years ($\approx$ 6205 days) (Wurdinger 1973)
$\bar{\mu}$	$8.8 \times 10^{-4} + 1/6205$ per day (ASR of 0.725)
μ_{spring}	$1.64 \times 10^{-3} + 1/6205$ per day (ASR of 0.55)
μ_{autumn}	$8.8 \times 10^{-4} + 1/6205$ per day (ASR of 0.725)
return rate	0.75 (return to breeding location annually)
H5N1 mortality	2/5 dead inoculated bar-headed geese within 6–7 days (Mongolia 2005 virus; Brown *et al.* 2008), 80% of inoculated geese within 8.7–12.9 days (Qinghai bar-headed H5N1 2005 virus) (Zhou *et al.* 2006)
epizootic duration	May–June 2005 (61 days) in Qinghai Lake (e.g. Chen *et al.* 2005; Zhou *et al.* 2006)
$\mu_{\text{H5N1},i}$	1.46×10^{-1} per day (80% death over 11 days)

the one-age group model. Using these functions, we checked that the model recovers the conservation of number of birds when setting death and birth to zero as expected. In addition, a null death rate (in all patches except the breeding patch) with a non-zero intrinsic growth rate in the breeding patch leads to the recovery of the logistic growth dynamics for the system of patches (see the electronic supplementary

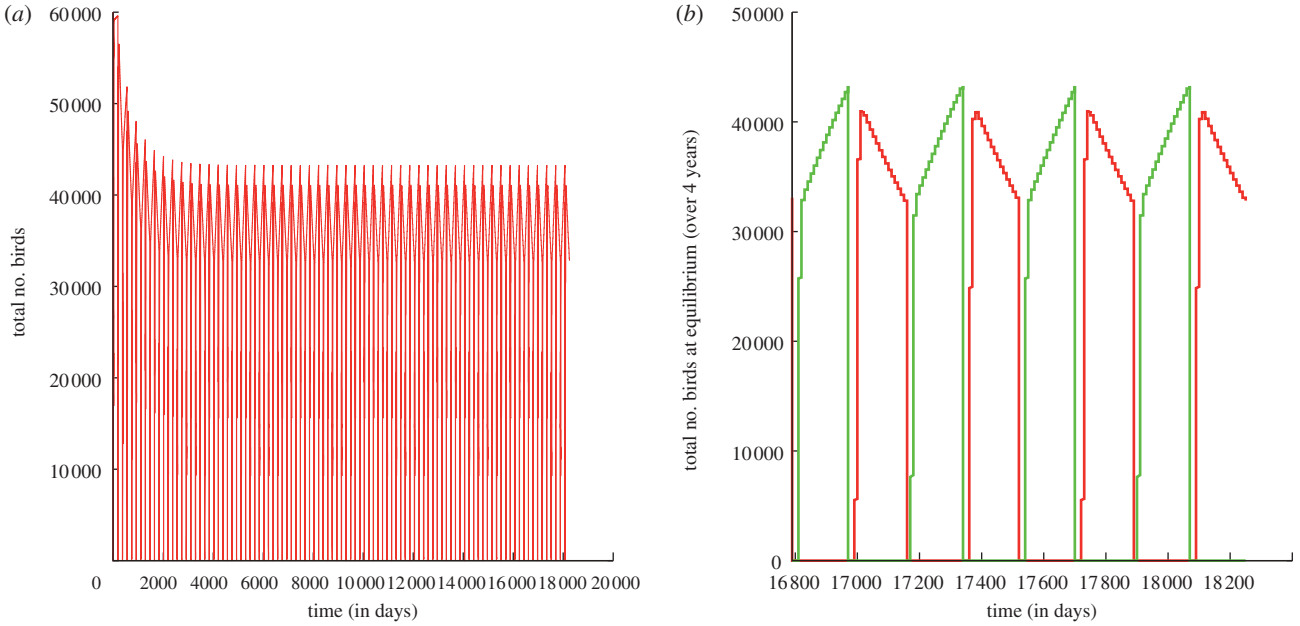

Figure 4. Over a simulation of 50 years, the bird population reaches an equilibrium value of 40 000 total bird population. The model equilibrium is reached for various initial conditions, for example (*a*) $\phi^0(0) = 60\,000$ and (*b*) the equilibrium population on the wintering and breeding grounds is shown over 4 years. (*a*) Red line, total population on stopovers. (*b*) Red line, population at wintering ground; green, population at breeding ground.

material). From the above parameters, we obtained a return to the breeding site of approximately 75 per cent for the birds which departed the previous year. Figure 4*a* shows the longer term evolution of the total bird population over 50 years starting from an initial population at the breeding ground-carrying capacity (e.g. 60 000). The equilibrium value is around 40 000 birds varying from 33 000 birds at the end of the wintering season to up to 43 000 birds at the end of the breeding season (figure 4*b*). This equilibrium is in the range of the estimated world population of bar-headed geese (30 000–60 000).

3.2. Why season matters

We now use the model studied thus far to investigate the impact of an anomalously high death rate during the migration at one of the stopover locations and its influence on the overall species dynamics if it were to be recurrent. The anomalously high death toll could be due to repeated local outbreaks of H5N1 as it is known that H5N1 is now endemic in many regions of the world (Center for Infectious Disease Research & Policy 2008).

In figure 5, the H5N1 disease induced death is introduced in various patches, starting from an equilibrium population of 34 000. For equal duration of residence (e.g. on P_4 and P_{11}), the average number of birds at equilibrium is higher when the disease occurs during the spring migration. The opposite result was expected and advanced in the literature (e.g. Schekkerman & Slaterus 2007). In order to assess the influence of the time of residence on the previous results, we perform similar simulations with imposing a fictitious residence time. From the data collected for the autumn and spring migrations, we obtain an average residence time of 7.58 days taken for each migration stopover ($m_{\text{average}} = 0.60754$). The resulting equilibrium population is shown in figure 6. Regardless of the location of the high death rate on the autumn migration route, the equilibrium is unchanged. Similarly, the equilibrium remains the same when changing the location of the infected patch on the spring route. However, the same death rate when introduced anywhere during the spring migration led to an average annual size of the equilibrium population that is higher than that when introduced in the autumn migration. The transition to this equilibrium is characterized by an opposite trend. In the first years of high death toll, the population appears to be more affected when the death toll is introduced on the autumn migration route, before reversing to an equilibrium where the opposite is true.

3.3. Role of age structure

For bar-headed geese, females do not reach maximum reproduction efficiency before age 4 (Wurdinger 1973; Lamprecht 1987). Because of this reproductive age and the higher death rate among young birds infected by H5N1 (Brown *et al.* 2008), it is important to understand the effect of age–structure on the internal migratory and reproductive dynamics of the flocks. We consider two age groups of birds: the adults A and the juveniles J. We assume an exponential transition for the juveniles with 99 per cent of the juveniles maturing by age 4, leading to a constant maturation rate of $\lambda = 3.15 \times 10^{-3}$ per day. Note that the reproductive maturation, in reality, spans a range of values from 2 to 4 years (table 3). Using a derivation analogous to that presented for the previous model, we arrive at the following system of delay differential

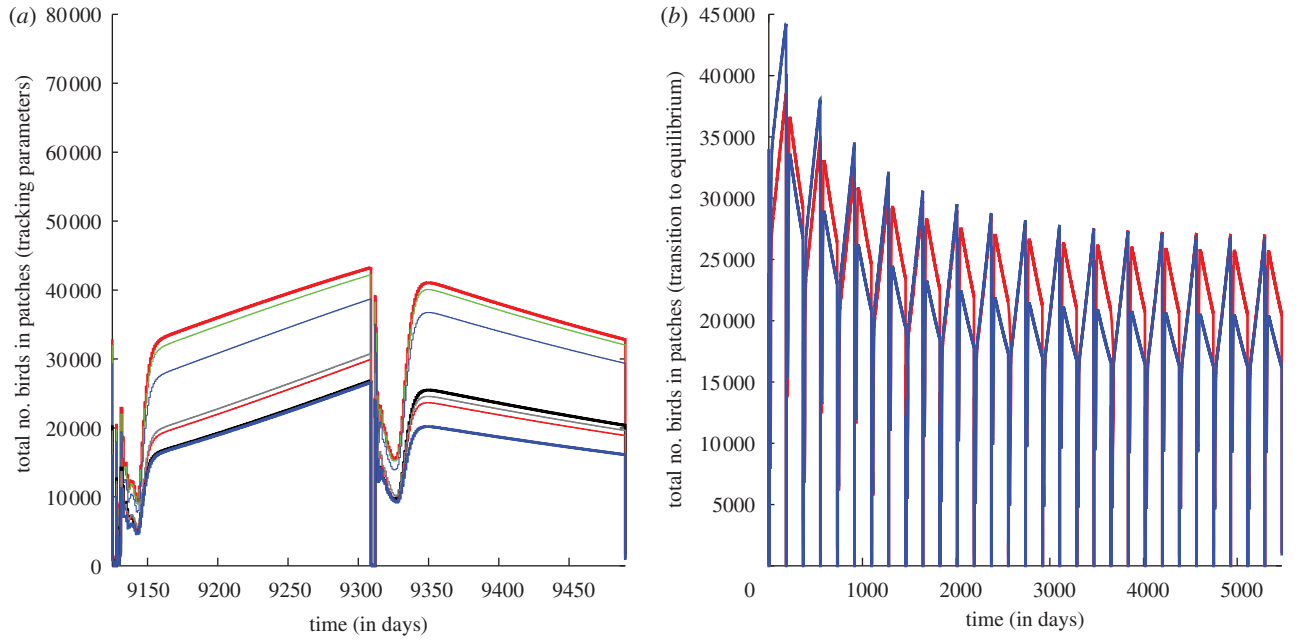

Figure 5. Time series of the total population (*a*) at equilibrium and (*b*) during transition to equilibrium after the introduction of repeated H5N1 disease induced death in patches of various residence time, starting from an equilibrium population of 34 000. (*a*) Thick red line, no H5N1; green line, disease on P_0; thin blue line, disease on P_1; black line, disease on P_4; thin red line, disease on P_9; grey line, disease on P_{10}; thick blue line, disease on P_{11}. (*b*) Red line, disease on P_4; blue line, disease on P_{11}.

equations for the density of birds A and J on each stopover:

$$\begin{aligned}
\dot{A}^0 &= m_0(t-\tau_0)\times(\mathrm{e}^{-\mu\tau_0}A^N(t-\tau_0)+J^N(t-\tau_0)\\
&\quad \mathrm{e}^{-\mu\tau_0}(1-\mathrm{e}^{-\lambda\tau_0}))+\lambda J^0-(m_1+\mu_{A0})A^0,\\
\dot{J}^0 &= \mathrm{e}^{-(\mu+\lambda)\tau_0}m_0(t-\tau_0)J^N(t-\tau_0)\\
&\quad -(m_1+\mu_{J0}+\lambda)J^0,\\
\dot{A}^1 &= m_1\times(\mathrm{e}^{-\mu\tau_1}A^0(t-\tau_1)+J^0(t-\tau_1)\mathrm{e}^{-\mu\tau_1}\\
&\quad (1-\mathrm{e}^{-\lambda\tau_1}))+\lambda J^1-(m_2+\mu_{A1})A^1,\\
\dot{J}^1 &= \mathrm{e}^{-(\mu+\lambda)\tau_1}m_1J^0(t-\tau_1)-(m_2+\mu_{J1}+\lambda)J^1,\\
&\vdots\\
\dot{A}^{N/2} &= m_{N/2}\times(\mathrm{e}^{-\mu\tau_{N/2}}A^{N/2-1}(t-\tau_{N/2})\\
&\quad +J^{N/2-1}(t-\tau_{N/2})\times\mathrm{e}^{-\mu\tau_{N/2}}\\
&\quad (1-\mathrm{e}^{-\lambda\tau_{N/2}}))+\lambda J^{N/2}-m_{N/2+1}(t)A^{N/2},\\
\dot{J}^{N/2} &= \mathrm{e}^{-(\mu+\lambda)\tau_{N/2}}m_{N/2}J^{N/2-1}(t-\tau_{N/2})\\
&\quad +B^*(J^{N/2},A^{N/2})-\lambda J^{N/2}-m_{N/2+1}(t)J^{N/2},\\
&\vdots\\
\dot{A}^N &= m_N\times(\mathrm{e}^{-\mu\tau_N}A^{N-1}(t-\tau_N)+J^{N-1}\\
&\quad (t-\tau_N)\mathrm{e}^{-\mu\tau_N}(1-\mathrm{e}^{-\lambda\tau_N}))+\lambda J^N\\
&\quad -(m_0(t)+\mu_{AN})A^N\\
\text{and}\quad \dot{J}^N &= \mathrm{e}^{-(\mu+\lambda)\tau_N}m_NJ^{N-1}(t-\tau_N)\\
&\quad -(m_0(t)+\mu_{JN}+\lambda)J^N, \qquad (3.1)
\end{aligned}$$

where the birth rate in the breeding patch is determined by the adult population and causes an increase in the juvenile population. We assume the death rates for the adults and juveniles to be equal on the flyways, but different on the stopovers

$$B^*(J^{N/2},A^{N/2})=\gamma A^{N/2}\left(1-\frac{J^{N/2}+A^{N/2}}{K}\right). \qquad (3.2)$$

The growth of the population only contributes to the increase in the population J on the breeding ground $P_{N/2}$, where the limiting density capacity is determined by both the adults and juveniles. On land, the survival rate of juveniles is taken to be 32 per cent in the spring and winter and 40 per cent in the autumn, while that of the adults is 72.5 per cent. Note that here we assume the same time scale for the reproductive and immune system maturation. How the difference between immune system maturation and reproduction maturation affects the disease dynamics and spatial spread of bird populations remains to be an interesting subject for future study.

The variations of death rates are due to the differences of body mass and immune resistance between juveniles and adults, which can be exacerbated by the seasonal changes of food distribution and temperature (Schekkerman & Slaterus 2007). The parameters selected give a return rate to the breeding patch after 1 year of 56 per cent for the juveniles and 83 per cent for adults. Starting with the above parameters and an initial population of 15 000 adults and 15 000 juveniles, we obtain an equilibrium population that varies between a high of 44 100 at the end of the summer (35 500 adults and 8600 juveniles) to a low of 36 000 at the end of the winter (33 000 adults and 3000 juveniles; see the electronic supplementary material). Next, the high H5N1 disease death rate is introduced at various locations similar to the previous model. Recall that Zhou *et al.* (2006) found an 80 per cent death

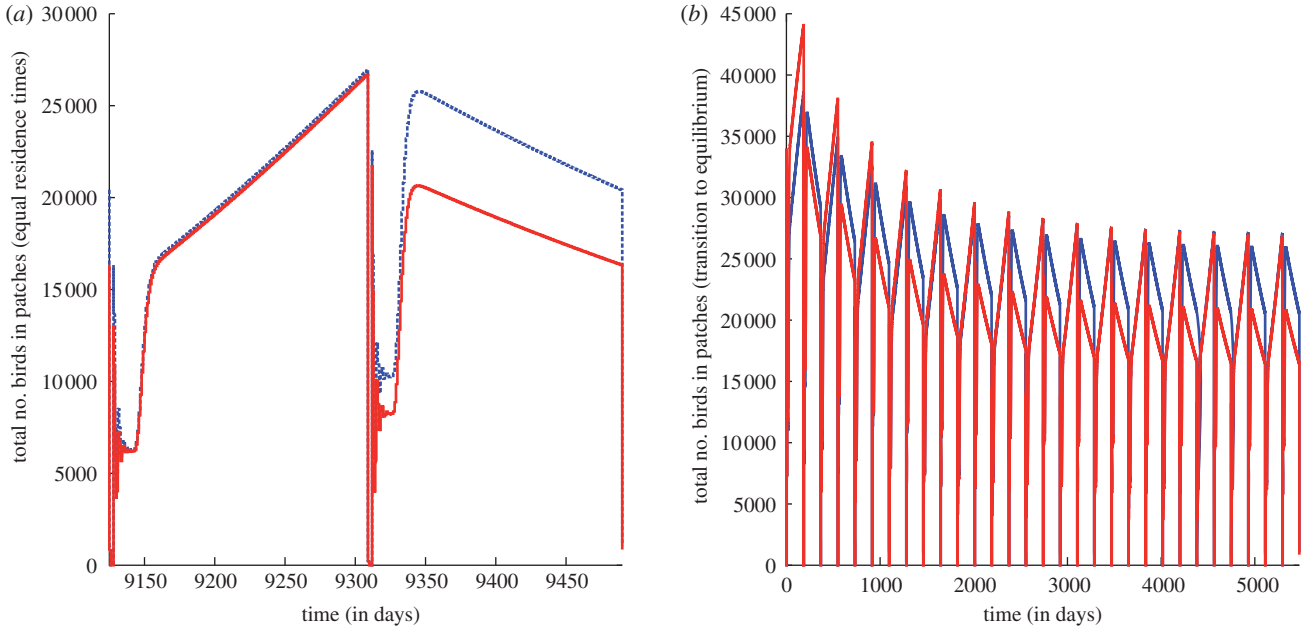

Figure 6. Time series of the total population on patches (*a*) at equilibrium and (*b*) during transition to equilibrium after the introduction of the repeated H5N1 disease-induced death in various patches of equal average residence time $m_{\text{average}} = 0.60754$, starting from an equilibrium population of 34 000. (*a*) Dashed blue line, disease in spring: P_{1-5}; red line, disease in autumn: P_{7-11}. (*b*) Blue line, disease in spring: P_{1-5}; red line, disease in autumn: P_{7-11}.

Table 3. Parameters of the two-age group model of juvenile and adult populations.

egg laying	average 5.3 per female with 34% average hatching success (Wurdinger 1973)
survival to 1 year	32% of hatched birds survive to one year of age (Wurdinger 1973)
γ	$4.99 \times 10^{-3}\,\text{d}^{-1}$
maturation age	2–4 years (maturation to highest reproduction rate in primary females; Wurdinger 1973; Lamprecht 1987)
λ	$3.15\times 10^{-3}\,\text{d}^{-1}$ (99% mature by age 4)
μ_A	$8.8 \times 10^{-4}\,\text{d}^{-1}$ on all patches (annual survival rate of 0.725)
$\mu_{J(\text{autumn})}$	$2.5 \times 10^{-3}\,\text{d}^{-1}$ on all patches (annual survival rate of 0.4)
$\mu_{J(\text{spring}-\text{winter})}$	$3.12 \times 10^{-3}\,\text{d}^{-1}$ on all patches (annual survival rate of 0.32)
μ	$8.8\times 10^{-4}\,\text{d}^{-1}$ during flight for all birds (annual survival rate of 0.725)
annual return rate to breeding location	
juvenile return rate	0.56
adult return rate	0.83
population return rate	0.7
$\mu_{J-\text{H5N1}}$	$1.46 \times 10^{-1}\,\text{d}^{-1}$ (80% death over 11 days) (see Zhou *et al.* (2006) for three-week-old geese)
$\mu_{A-\text{H5N1}}$	$4.6\times 10^{-2}\,\text{d}^{-1}$ (40% death rate over 11 days) (see Brown *et al.* (2008) for older geese of about 12 weeks)

rate for three-week-old geese, while the experiment of Brown *et al.* (2008) found a death rate of 40 per cent, although their sample was limited. Note that the geese used in the experiment of Brown *et al.* (2008) were older at 12 weeks old. We do not have death rates from the literature specifically for the adult bar-headed geese infected by H5N1; however, we rely on these studies to set a death rate of 80 per cent for the juveniles and 40 per cent for the adults in the simulations presented herein.

Figure 7 shows the impact of the H5N1 death toll on the bird population depending on the location of the disease. The population at equilibrium is shown in figure 7*a* and its transition to the equilibrium is shown in figure 7*b*. These results were obtained starting from an equilibrium population of 33 000 adults and 3000 juveniles. We recover that the effect on the population equilibrium is more severe when the H5N1 death toll is introduced during the autumn migration (patches 7–11) compared with when it is introduced in the spring migration (patches 1–5). This begins to be true only after a few years of adjustment as shown in figure 7*b*. At equilibrium, the difference in the size of the populations subjected to repeated spring outbreaks (denoted S) and those subjected to repeated autumn outbreaks (denoted F) appears in both adult and juvenile sub-populations.

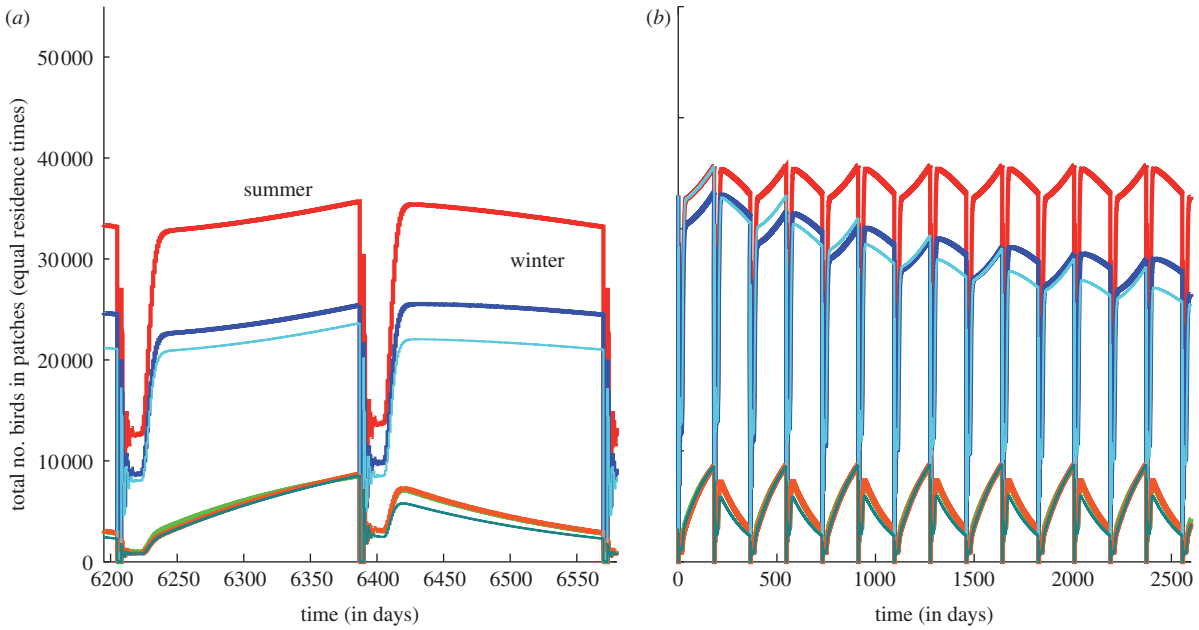

Figure 7. Time series of the adult and juvenile bird populations on patches (*a*) at equilibrium and (*b*) during transition to equilibrium for repeated H5N1 induced death in either a spring or autumn migration patch when starting from an equilibrium population of 33 000 adults and 3000 juveniles and with the fictitious residence time on each stopover corresponding to $m_{\text{average}} = 0.60754$. Red line, no H5N1: adults; light green line, no H5N1: juveniles; dark blue line, disease in spring: adults; orange line, disease in spring: juveniles; light blue line, disease in autumn: adults; grey line, disease in autumn: juveniles.

Figure 7 shows that the difference between the number of juveniles in populations S and F is significant in the winter, while being of similar size in the summer. This is true after only 1 year. The adult population shows a similar difference in size between populations S and F early on, but eventually reaches the equilibrium, where the difference in the number of adults between populations S and F is apparent all year long. The smaller number of juveniles in the winter for population F influences the number of adults in the spring and summer. In sum, the two-age model shows that repeated outbreaks in the autumn lead to a reduced number of juveniles arriving at the wintering ground. During the winter, there are larger losses of juveniles, which in turn affects the equilibrium size of the adult population in the spring. Fewer adults arrive at the breeding ground, resulting in a smaller total population repeatedly affected by H5N1 in the autumn.

4. DISCUSSION

We found that repeated deadly epizootics of H5N1 at stopovers during the autumn migration would cause more losses to the affected population over time than repeated epizootics during the spring migration. This is observed when the populations of birds reach their new equilibrium size in response to the repeated outbreaks. In addition, this is observed in both the one-age-group and two-age-group models. However, during the early years of adjustment to the outbreaks, the opposite is true. In other words, during the first few years, the population of the group repeatedly affected by H5N1 in the spring is smaller than that repeatedly affected in the autumn. This finding is counter-intuitive, especially when considering that we accounted for the higher reported natural death rate of birds during the spring migration compared with that during the autumn migration. The reversal of dynamics during the transition to equilibrium was not expected and shows that the intuitive assessment of the impact of repeated autumn outbreaks discussed in the literature is valid, but only for the early years.

In order to investigate further the effect of repeated outbreaks on bird species and examine the possible role of the birds in the local or non-local spread of H5N1, improvements to the present modelling efforts need to be made. These include a more complex modelling of the disease outbreak dynamics and the inclusion of the role of the aquatic environment in keeping some stopovers contaminated (Brown *et al.* 2009). In fact, we did not incorporate the effect of environmental transmission of the avian influenza viruses on the stopovers which could prove important in the maintenance of the outbreaks from one year to the next as was highlighted by Breban *et al.* (2009) for the case of the LPAI virus. As such, the results in the present study are a first step towards the ultimate goal of better understanding the complex dynamics of the spread of H5N1 and its impact on vulnerable species of wild birds. Finally, the model presented here has the advantage of flexibility, allowing one to incorporate shifted migration times and their impact on the introduction of HPAI viruses and spread between stopovers. This is of relevance for the estimation of the impact of climate change on modifying the migration and hence disease dynamics as highlighted recently (e.g. Hdenström 2008; Carey 2009).

LB and JW acknowledge supports from Natural Sciences and Engineering Research Council of Canada, the Shared Hierarchical Academic Research Network, the Mathematics

of Information Technology and Complex Systems, the Geomatics for Informed Decisions, the Public Health Agency of Canada and the National Research Council of Canada and thank the three anonymous referees for their constructive comments. The other co-authors would like to acknowledge funding support from the FAO; USGS Avian Influenza Program; Bangor University, Biotechnology and Biological Sciences Research Council; and the Max Planck Institute for Ornithology; and investigators D. Douglas, W. Perry, A. Schultz, and S. Schwarzbach (USGS); P. Frappell (Univ. Tasmania); W. Milsom (Univ. British Columbia); and G. Scott (Univ. St. Andrews). This study followed the recommendations of a USGS Animal Care and Use Committee, and we thank K. Phillips and R. Kirby for an expedited policy review. Use of any trade names does not imply U.S. government endorsement.

REFERENCES

Akesson, S. & Hedenström, A. 2007 How migrants get there: migratory performance and orientation. *BioScience* **52**, 123–133. (doi:10.1641/B570207)

Alerstam, T. 2006 Conflicting evidence about long-distance animal navigation. *Science* **313**, 791–794. (doi:10.1126/science.1129048)

Alerstam, T., Gudmundsson, G. A., Green, M. & Hedenström, A. 2001 Migration along orthodromic sun compass routes by arctic birds. *Science* **291**, 300–303. (doi:10.1126/science.291.5502.300)

Alexander, D. J. 2000 A review of avian influenza in different bird species. *Vet. Microbiol.* **74**, 3–13. (doi:10.1016/S0378-1135(00)00160-7)

Avian Influenza Wildlife & The Environment Web. 2008 Wildlife conservation implications. See http://www.aiweb.info/document.aspx?DocID=358#9.

Barta, Z., McNamara, J. M., Houston, A. I., Weber, T. P., Hedenström, A. & Feró, O. 2008 Optimal moult strategies in migratory birds. *Phil. Trans. R. Soc. B* **363**, 211–229. (doi:10.1098/rstb.2007.2136)

Bauer, S., Gienapp, P. & Madsen, J. 2008 The relevance of environmental conditions for departure decision changes en route in migrating geese. *Ecology* **89**, 1953–1960. (doi:10.1890/07-1101.1)

Bird Life International. 2009 Species factsheet: *Anser indicus*. See http://www.birdlife.org.

Both, C. & Visser, M. E. 2005 The effect of climate change on the correlation between avian life-history traits. *Glob. Change Biol.* **11**, 1606–1613. (doi:10.1111/j.1365-2486.2005.01038.x)

Breban, R., Drake, J. M., Stallknecht, D. E. & Rohani, P. 2009 The role of environmental transmission in recurrent avian influenza epidemics. *PLoS Comput. Biol.* **5**, e1000346-1. (doi:10.1371/journal.pcbi.1000346)

Brown, J. D., Swayne, D. E., Cooper, R. J., Burns, R. E. & Stallknecht, D. E. 2007 Persistence of H5 and H7 avian influenza viruses in water. *Avian Dis.* **51**, 285–289. (doi:10.1637/7636-042806R.1)

Brown, J. D., Stallknecht, D. E. & Swayne, D. E. 2008 Experimental infection of swans and geese with highly pathogenic avian influenza virus (H5N1) of Asian lineage. *Emerg. Infect. Dis.* **14**, 136–142. (doi:10.3201/eid1401.070740)

Brown, J. D., Goekjian, G., Poulson, R., Valeika, S. & Stallknecht, D. E. 2009 Avian influenza virus in water: infectivity is dependent on pH, salinity and temperature. *Vet. Microbiol.* **136**, 20–26. (doi:10.1016/j.vetmic.2008.10.027)

Carey, C. 2009 The impacts of climate change on the annual cycles of birds. *Phil. Trans. R. Soc. B* **364**, 3321–3330. (doi:10.1098/rstb.2009.0182)

Center for Infectious Disease Research & Policy. 2008 Egyptian teen dies of H5N1 infection. See http://www.cidrap.umn.edu/cidrap/content/influenza/avianflu/news/dec1608egypt-jw.html.

Center for Infectious Disease Research & Policy. 2009 Four new cases push H5N1 total past 400. See http://www.cidrap.umn.edu/cidrap/content/influenza/avianflu/news/jan2609humans-br.html.

Chen, H. *et al.* 2004 The evolution of H5N1 influenza viruses in ducks in southern China. *Proc. Natl Acad. Sci. USA* **101**, 10 452–10 457. (doi:10.1073/pnas.0403212101)

Chen, H., Smith, G. J. D., Zhang, S. Y., Qin, K., Wang, J., Li, K. S., Webster, R. G., Peiris, J. S. M. & Guan, Y. 2005 Avian flu: H5N1 virus outbreak in migratory waterfowl. *Nature* **436**, 191–192. (doi:10.1038/nature03974)

Chen, H. *et al.* 2006*a* Properties and dissemination of H5N1 viruses isolated during an influenza outbreak in migratory waterfowl in western China. *J. Virol.* **80**, 5976–5983. (doi:10.1128/JVI.00110-06)

Chen, H. *et al.* 2006*b* Establishment of multiple sublineages of H5N1 influenza virus in Asia: implications for pandemic control. *Proc. Natl Acad. Sci. USA* **103**, 2845–2850. (doi:10.1073/pnas.0511120103)

Cui, P. *et al.* 2010 Movement patterns of Bar-headed Geese Anser indicus during breeding and post-breeding periods in Qinghai Lake, China. *J. Ornithology.*

Dolman, P. M. & Sutherland, W. J. 1994 The response of bird populations to habitat loss. *Ibis* **137**, S38–S46. (doi:10.1111/j.1474-919X.1995.tb08456.x)

Feare, C. J. & Yasué, M. 2006 Asymptomatic infection with highly pathogenic avian influenza H5N1 in wild birds: how sound is the evidence? *Virol. J.* **96**, 1–4.

Gilbert, M., Xiao, X., Domenech, J., Lubroth, J., Martin, V. & Slingenbergh, J. 2006 Anatidae migration in the western Palearctic and spread of highly pathogenic avian influenza H5N1 virus. *Emerg. Infect. Dis.* **12**, 1650–1656.

Gudmundsson, G. A. & Alerstam, T. 1998 Optimal map projections for analysing long-distance migration routes. *J. Avian Biol.* **29**, 597–605. (doi:10.2307/3677180)

Hasselquist, D., Lindström, A., Jenni-Eiermann, S., Koolhaas, A. & Piersma, T. 2007 Long flights do not influence immune responses of a long distance migrant bird: a wind tunnel experiment. *Exp. Biol.* **210**, 1123–1131. (doi:10.1242/jeb.02712)

Haydon, D. T., Cleaveland, S., Taylor, L. H. & Laurenson, M. K. 2002 Identifying reservoirs of infection: a conceptual and practical challenge. *Emerg. Infect. Dis.* **8**, 1468–1473. (doi:10.3201/eid0812.010317)

Hdenström, A. 2008 Adaptations to migration in birds: behavioural strategies, morphology and scaling effects. *Phil. Trans. R. Soc. B* **363**, 287–299. (doi:10.1098/rstb.2007.2140)

Javed, S., Takekawa, D. C., Douglas, A. R., Rahmani, Y., Kanai, M., Nagendran, B. C. C. & Sharma, S. 2000 Tracking the spring migration of a Bar-headed goose (*Anser indicus*) across the Himalaya with satellite telemetry. *Glob. Environ. Res.* **4**, 195–205.

Kilpatrick, A. M., Chmura, A. A., Gibbons, D. W., Fleischer, R. C., Marra, P. P. & Daszak, P. 2008 Predicting the global spread of H5N1 avian influenza. *Proc. Natl Acad. Sci. USA* **103**, 19 368–19 373. (doi:10.1073/pnas.0609227103)

Kokko, H. 1999 Competition for early arrival in migratory birds. *J. Anim. Ecol.* **68**, 940–950. (doi:10.1046/j.1365-2656.1999.00343.x)

Kuiken, T., Rimmelzwaan, G., van Riel, D., van Amerongen, G., Baars, M., Fouchier, R. & Osterhaus, A. 2004 Avian H5N1 influenza in cats. *Science* **306**, 241. (doi:10.1126/science.1102287)

Lamprecht, J. 1987 Female reproductive strategies in bar-headed geese (*Anser indicus*): why are geese monogamous? *Behav. Ecol. Sociobiol.* **21**, 297–305. (doi:10.1007/BF00299967)

Lebarbenchon, C. *et al.* 2009 Spread of avian influenza viruses by common teal (*Anas crecca*) in Europe. *PLoS ONE* **4**, e7289. (doi:10.1371/journal.pone.007289)

Lipatov, A. S. *et al.* 2007 Influenza (H5N1) viruses in poultry, Russian Federation, 2005–2006. *Emerg. Infect. Dis.* **13**, 539–546. (doi:10.3201/eid1304.061266)

Liu, J. *et al.* 2005 Highly pathogenic H5N1 influenza virus infection in migratory birds. *Science* **309**, 1206. (doi:10.1126/science.1115273)

Madsen, J., Frederiksen, M. & Ganter, B. 2002 Trends in annual and seasonal survival of pink-footed geese *Anser brachyrhynchus*. *Ibis* **144**, 218–226. (doi:10.1046/j.1474-919X.2002.00045.x)

Olsen, B., Munster, V. J., Wallensten, A., Waldenström, J., Osterhaus, A. D. M. E. & Fouchier, R. A. M. 2006 Global pattern of influenza A in wild birds. *Science* **312**, 384–388. (doi:10.1126/science.1122438)

Prins, H. H. T. & van Wieren, S. E. 2004 Number, population structure and habitat use of bar-headed geese *Anser indicus* in Ladakh (India) during the brood-rearing period. *Acta Zool. Sin.* **50**, 738–744.

Reperant, L. A., van Amerongen, G., van de Bildt, M. W. G., Rimmelzwaan, G. F., Dobson, A. P., Osterhaus, A. D. M. E. & Kuiken, T. 2008 Highly pathogenic avian influenza virus (H5N1) infection in red foxes fed infected bird carcasses. *Emerg. Infect. Dis.* **14**, 1835–1841. (doi:10.3201/eid1412.080470)

Schekkerman, H. & Slaterus, R. 2007 British Trust for Ornithology-Web. Population dynamics and prevalence of influenza A viruses in mallard, mute swan and other wildfowl. See http://www.bto.org/ai/pdfs/mortality-review070623_1_.pdf.

Si, Y., Skidmore, A. K., Wang, T., de Boer, W. F., Debba, P., Toxopeus, A. G., Li, L. & Prins, H. H. T. 2009 Spatio-temporal dynamics of global H5N1 outbreaks match bird migration patterns. *Geospatial Health* **4**, 65–78.

Stöhr, K. 2005 Avian influenza and pandemics—research needs and opportunities. *N. Engl. J. Med.* **352**, 405–407. (doi:10.1056/NEJMe048344)

Takekawa, J. Y. *et al.* 2010 Migration of waterfowl in the East Asian Flyway and spatial relationship to HPAI H5N1 outbreaks. *Avian Dis.* **53**, 466–476. *Wildfowl* **59**, 102–125.

Ungchusak, K. *et al.* 2005 Probable person-to-person transmission of avian influenza A (H5N1). *N. Engl. J. Med.* **352**, 333–340. (doi:10.1056/NEJMoa044021)

van Gils, J. A., Munster, V. J., Radersma, R., Liefhebber, D., Fouchier, R. A. M. & Klaassen, M., 2007 Hampered foraging and migratory performance in swans infected with low-pathogenic avian influenza A virus. *PLoS ONE* **2**, e184. (doi:10.1371/journal.pone.0000184)

Ward, D. H., Rexstad, E. A., Sedinger, J. S., Lindberg, M. S. & Dawe, N. K. 1997 Seasonal and annual survival of adult Pacific brant. *J. Wildlife Manage.* **61**, 773–781. (doi:10.2307/3802184)

Weber, T. P. & Stilianakis, N. 2007 Ecologic immunology of avian influenza (H5N1) in migratory birds. *Emerg. Infect. Dis.* **13**, 1139–1143.

Weber, T. P., Ens, B. J. & Houston, A. I. 1998 Optimal avian migration: a dynamic model of fuel stores and site use. *Evol. Ecol.* **12**, 377–401. (doi:10.1023/A:1006560420310)

Webster, R., Bean, W. J., Gorman, O. T., Chambers, T. M. & Kawaoka, Y. 1992 Evolution and ecology of influenza A viruses. *Macrobiol. Rev.* **56**, 152–179.

World Health Organization. 2005 Avian influenza frequently asked questions. See http://www.who.int/csr/disease/avian_influenza/avian_faqs/en/print.html.

World Health Organization. 2008 Avian influenza: situation in Pakistan—update 2. See http://www.who.int/csr/don/2008_04_03/en/index.html.

World Health Organization. 2009*a* Cumulative number of confirmed human cases of avian influenza A/(H5N1) reported to WHO. See http://www.who.int/csr/disease/avian_influenza/country/cases_table_2009_01_26/en/index.html.

World Health Organization. 2009*b* Epidemic and pandemic alert and response. H5N1 avian influenza: timeline of major events. See http://www.who.int/csr/disease/avian_influenza/ai_timeline/en/.

Wurdinger, I. 1973 Breeding of bar-headed geese *Anser indicus* in captivity. *Int. Zoo Yearbook* **13**, 43–47. (doi:10.1111/j.1748-1090.1973.tb02100.x)

Yasué, M., Feare, C. J., Bennun, L. & Fiedler, W. 2006 The epidemiology of H5N1 avian influenza in wild birds: why we need better ecological data. *BioScience* **56**, 923–929. (doi:10.1641/0006-3568(2006)56[923:TEOHAI]2.0.CO;2)

Zhou, J.-Y., Shen, H.-G., Chen, H.-X., Tong, G.-Z., Liao, M., Yang, H.-C. & Liu, J.-X. 2006 Characterization of a highly pathogenic H5N1 influenza virus derived from bar-headed geese in China. *J. Gen. Virol.* **87**, 1823–1833. (doi:10.1099/vir.0.81800-0)